

# Journal of Materials Chemistry A

Accepted Manuscript



This is an *Accepted Manuscript*, which has been through the Royal Society of Chemistry peer review process and has been accepted for publication.

*Accepted Manuscripts* are published online shortly after acceptance, before technical editing, formatting and proof reading. Using this free service, authors can make their results available to the community, in citable form, before we publish the edited article. We will replace this *Accepted Manuscript* with the edited and formatted *Advance Article* as soon as it is available.

You can find more information about *Accepted Manuscripts* in the [Information for Authors](#).

Please note that technical editing may introduce minor changes to the text and/or graphics, which may alter content. The journal's standard [Terms & Conditions](#) and the [Ethical guidelines](#) still apply. In no event shall the Royal Society of Chemistry be held responsible for any errors or omissions in this *Accepted Manuscript* or any consequences arising from the use of any information it contains.

# Evolution of the electrochemical capacitance of transition metal oxynitrides with time: effect of ageing and passivation

Cite this: DOI: 10.1039/x0xx00000x

Received 00th January 2014,  
Accepted 00th January 2014

DOI: 10.1039/x0xx00000x

www.rsc.org/

Olga Kartachova,<sup>a</sup> Ying Chen,<sup>a</sup> Robert Jones,<sup>b</sup> Yanhui Chen,<sup>c</sup> Hongzhou Zhang,<sup>c</sup> and Alexey M. Glushenkov<sup>\*a,d</sup>

A number of transition metal nitrides and oxynitrides, which are actively investigated today as electrode materials in a wide range of energy conversion and storage devices, possess an oxide layer on the surface. Upon exposure to the ambient air, properties of this layer progressively change, in the process known as “ageing”. Since a number of electrochemical processes involve the surface or sub-surface layers of the active electrode compounds only, ageing could have a significant effect on the overall performance of energy conversion and storage devices. In this work, the influence of the ageing of tungsten and molybdenum oxynitrides on their electrochemical properties in supercapacitors is explored for the first time. Samples are synthesised by the temperature-programmed reduction in  $\text{NH}_3$  and are treated with different gases prior exposure to air in order to evaluate the role of the passivation in the ageing process. After the synthesis, products are subjected to the controlled ageing and are characterised by the low temperature nitrogen adsorption, X-ray photoelectron spectroscopy and transmission electron microscopy. Capacitive properties of the compounds are evaluated by performing cyclic voltammetry and galvanostatic charge and discharge measurements in 1M  $\text{H}_2\text{SO}_4$  electrolyte.

## 1. Introduction

In the recent years, transition metal nitrides and oxynitrides have been widely investigated as candidates for applications in the energy conversion and storage devices due to unique physico-chemical properties such as high intrinsic conductivity, electrochemical and Pt-like electrocatalytic activity, as well as the resistance to corrosion.<sup>1-36</sup> The range of devices they can be potentially used in includes lithium-ion batteries, electrochemical supercapacitors, dye-sensitised solar cells, metal-air batteries and fuel cells. For instance, compounds such as  $\text{CrN}$ ,<sup>2</sup>  $\text{CoN}$ ,<sup>3,4</sup> and  $(\text{Ni}_{0.33}\text{Co}_{0.67})\text{N}$ <sup>5</sup> nanoparticles as well as thin films of  $\text{VN}$ ,<sup>6</sup>  $\text{CrN}$ ,<sup>7</sup>  $\text{Co}_3\text{N}$ ,<sup>8</sup>  $\text{Fe}_3\text{N}$ ,<sup>8</sup>  $\text{RuN}$ ,<sup>9</sup>  $\text{Mn}_3\text{N}_2$ <sup>10</sup> and  $\text{V}_2\text{ON}$ <sup>11</sup> have demonstrated reversible capacity values between  $323 \text{ mA h g}^{-1}$  for  $\text{Fe}_3\text{N}$ <sup>8</sup> and  $1200 \text{ mA h g}^{-1}$  for  $\text{CrN}$ <sup>7</sup> through a conversion reaction mechanism as anode materials for lithium-ion batteries. In supercapacitors, transition metal nitrides and oxynitrides have shown good rate capabilities, as opposed to many transition metal oxides which suffer from poor intrinsic conductivity, with typical specific capacitance values between

$30$  and  $350 \text{ F g}^{-1}$ .<sup>9,12-26</sup>  $\text{MoW}(\text{N},\text{O})$  has demonstrated the ability to operate at a current as high as  $20 \text{ A g}^{-1}$ , still retaining 43% of its initial capacitance measured at  $0.05 \text{ A g}^{-1}$ ,<sup>14</sup> while  $\text{TiN-VN}$  core-shell mesoporous fibres have retained 64% of the initial capacitance upon increasing the current load from 2 to  $10 \text{ A g}^{-1}$ .<sup>15</sup> Dye-sensitised solar cells with electrocatalytic counter-electrodes containing  $\text{Mo}_2\text{N}$ ,<sup>27</sup>  $\text{W}_2\text{N}$ ,<sup>27</sup>  $\text{VN}$ ,<sup>28</sup>  $\text{MoN}$ ,<sup>29</sup>  $\text{WN}$ <sup>29</sup> or  $\text{Fe}_2\text{N}$ <sup>29</sup> have shown up to 92% of the photovoltaic performance of the solar cells with platinum counter-electrodes.<sup>27-29</sup> Furthermore,  $\text{TiN}$ ,<sup>30-32</sup>  $\text{TaO}_x\text{N}_y$ ,<sup>33</sup>  $\text{CoWON}$ ,<sup>34</sup>  $\text{Mo}(\text{N},\text{O})$ <sup>35</sup> and  $\text{Co}_3\text{Mo}_3\text{N}$ <sup>36</sup> appear promising as electrocatalysts for the oxygen reduction reaction.

In the energy conversion and storage devices, a number of electrochemical and electrocatalytic processes such as the pseudocapacitive charge storage or oxygen reduction reaction often involve the surface or sub-surface layers of the active electrode materials. In fact, it has been proposed that the origin of the specific capacitance of vanadium nitride could be attributed to the presence of vanadium oxides or oxynitrides on the surface, which participate in Faradaic processes with ions

from the electrolyte.<sup>26</sup> Furthermore, the mechanism of the oxygen reduction reaction is influenced by the presence of the active sites for O<sub>2</sub> adsorption and water desorption on the surface of the nitride or oxynitride electrocatalyst.<sup>32-34</sup> The properties and composition of the surface are therefore critical for the performance of these compounds as electrode materials.

It has been demonstrated, in the field of catalysis, that a number of transition metal nitrides and oxynitrides possess an oxide layer on the surface and properties of this layer are changing with time.<sup>37-39</sup> For instance, the surface of the passivated tungsten oxynitride becomes progressively covered with tungsten trioxide WO<sub>3</sub> upon exposure to air.<sup>37</sup> Furthermore, in the case of molybdenum oxynitrides,<sup>38,39</sup> an increase of the oxygen content has been revealed by the chemical analysis<sup>38,39</sup> or X-ray photoelectron spectroscopy (XPS) measurements<sup>39</sup> after storing the samples in the ambient air. Interestingly, no variations in the bulk structure of the materials have been detected on the X-ray diffraction (XRD) spectra,<sup>37-39</sup> indicating that ageing involves the surface or sub-surface layers only. This evolution of the surface composition of transition metal nitrides and oxynitrides with time remains almost unexplored in the field of the energy conversion and storage devices. Despite the promise of these materials, there are no studies, to the best of our knowledge, correlating ageing of nitrides and oxynitrides with changes in their electrochemical properties.

Furthermore, a number of these compounds are usually passivated (*i.e.* exposed to a stream of a gas containing a small amount of oxygen) prior the exposure to air in order to form a protective oxide layer and avoid the strong oxidation of the surface. The role of the passivation in the ageing process is not understood well, and the changes in the passivated materials remain largely unknown. It is, in our view, important to investigate the influence of the ageing and passivation on the electrochemical properties of transition metal nitrides and oxynitrides in order to determine the optimal synthesis and storage conditions, as changes of the surface properties could have an influence on their performance in the energy conversion and storage devices. Such a study may also be relevant to other related materials such as transition metal carbides, which have physico-chemical properties similar to nitrides and are also emerging as promising electrode materials. For example, transition metal carbide electrodes have been recently reported to have impressive capacitances in supercapacitors,<sup>40</sup> with volumetric capacitance values exceeding those for the activated graphene electrodes.

In this article, the influence of the ageing is investigated by comparing the performance of the fresh and aged molybdenum and tungsten oxynitrides as electrode materials in supercapacitors. Molybdenum and tungsten oxynitrides are synthesised by a temperature-programmed reduction in ammonia gas and exposed to the ambient air for different periods. In order to study the role of the passivation in the aging process, passivated and non-passivated tungsten oxynitrides are produced. Samples are characterised by the low temperature nitrogen (N<sub>2</sub>) adsorption, X-ray photoelectron spectroscopy

(XPS) and transmission electron microscopy (TEM). Effect of the ageing on the electrochemical performance in supercapacitors is evaluated by performing cyclic voltammetry and galvanostatic charge and discharge measurements in 1M H<sub>2</sub>SO<sub>4</sub> solution.

## 2. Experimental

### 2.1 Synthesis

Molybdenum and tungsten oxynitride samples were prepared by a temperature-programmed reduction of the corresponding oxide precursors (MoO<sub>3</sub> and WO<sub>3</sub>, respectively). The detailed temperature-programmed reduction procedure is described elsewhere.<sup>35</sup> In brief, 0.5g of the oxide precursor were heated in ammonia flow (0.2 l min<sup>-1</sup>). The temperature was raised to 700 °C at a rate of 3 °C min<sup>-1</sup> and kept stable for 2h. Subsequently, the sample was allowed to cool down to room temperature while the ammonia flow was maintained. The synthesised samples are further denoted as Mo(N,O) and W(N,O). In the present experiment, the synthesised molybdenum and tungsten oxynitride samples were treated with high-purity Ar (Coregas) prior the exposure to air during one hour. In order to study the effect of the room temperature oxidation (ageing), the synthesised samples were stored in open containers for periods up to 48 days in a drawer of a cabinet in the laboratory. Additionally, to evaluate the influence of the passivation on the ageing of the oxynitrides and its effect on the electrochemical properties, some synthesised tungsten oxynitride samples are passivated with a special gas mixture (Ar + 0.1 vol.% O<sub>2</sub>) during one hour prior the exposure to air.

Table 1. Description of tungsten oxynitride (W0-W48, WP0-WP48) and molybdenum oxynitride (Mo0-Mo48) samples exposed to the air for different periods.

Sample	Storage period (days)	Sample	Storage period (days)	Sample	Storage period (days)
W0	0 (fresh)	Mo0	0 (fresh)	WP0	0 (fresh)
W5	5	Mo21	21	WP5	5
W21	21	Mo35	35	WP21	21
W48	48	Mo48	48	WP48	48

Table 2. Weight of the active materials on tungsten oxynitride (W0-W48, WP0-WP48) and molybdenum oxynitride (Mo0-Mo48) electrodes.

Sample	Weight of the active material* (mg)	Sample	Weight of the active material (mg)	Sample	Weight of the active material (mg)
W0	2.38	Mo0	2.33	WP0	2.14
W5	2.31	Mo21	2.35	WP5	2.02
W21	2.32	Mo35	2.36	WP21	2.27
W48	2.4	Mo48	2.48	WP48	2.02

\* Total measurement uncertainty is 0.035 mg

Samples W0-W48 correspond to the non-passivated tungsten oxynitride and the samples Mo0-Mo48 correspond to the non-passivated molybdenum oxynitride, exposed to the ambient air for different periods. Samples WP0-WP48 denote the passivated tungsten oxynitride (refer to Table 1).

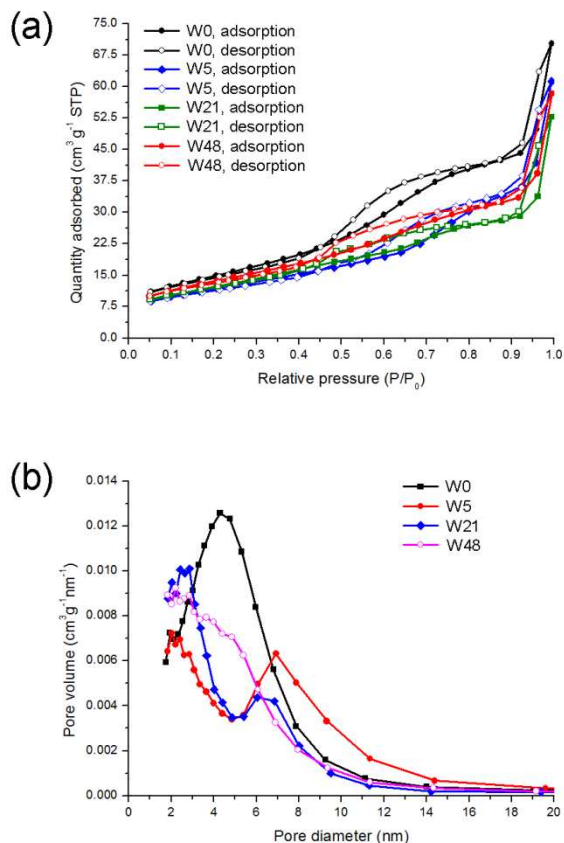


Figure 1. Nitrogen adsorption and desorption isotherms (a) and pore size distributions (b) for the non-passivated tungsten oxynitride samples.

## 2.2 Nitrogen adsorption and TEM analysis

Low temperature nitrogen adsorption measurements were performed on powder samples using Micromeritics Tristar 3000. The surface area was calculated from the low temperature adsorption isotherm by Branauer-Emmett-Teller (BET) method. Pore size distribution was evaluated using Barrett-Joiner-Helenda (BJH) method. TEM characterisation was performed with an FEI Titan, operating at the accelerating voltage of 300 kV. Energy filtered TEM (EFTEM) imaging was performed using the three window method.

## 2.3 Electrochemical testing

Electrochemical performance of the samples in supercapacitors was evaluated by cyclic voltammetry and galvanostatic charge and discharge experiments in 1M H<sub>2</sub>SO<sub>4</sub> electrolyte. Electrodes were prepared by coating a slurry, composed of the active material (90 wt. %), carbon nanopowder (Sigma-Aldrich, #699632) (5 wt. %), poly(vinylidene)fluoride (PVDF, Sigma-

Aldrich) (5 wt. %) and N-methyl-2-pyrrolidone (NMP, Sigma-Aldrich, anhydrous, 99.5 %) as a solvent, onto titanium foils. The coated foils were dried in vacuum at 90°C in the conventional oven overnight. Pt wires were used as counter electrodes and Ag/AgCl electrodes were used as reference electrodes. The electrochemical cells were filled with electrolyte under vacuum. In order to accurately compare the cyclic voltammetry measurements of the samples, electrodes with nearly identical weights were selected (Table 2).

## 2.4 XPS analysis

Prior to the use of electrodes in the electrochemical experiments, X-ray photoelectron spectra were acquired from the electrodes with a Kratos AXIS Nova instrument (Kratos Analytical Ltd, Manchester, UK) equipped with a monochromated Al K $\alpha$  X-ray source ( $h\nu = 1486.6$  eV) operating at 150 W. Mo 3d and W 4f spectra were recorded at a pass energy of 20 eV and 0.1 eV/step. The pressure was below 6E-9 torr. The binding energy measured for the dominant component of the C 1s photoemission was 284.4 eV, which is typical of graphitic carbon.<sup>41</sup>

## 3. Results

### 3.1 Characterisation and electrochemical properties of the non-passivated tungsten and molybdenum oxynitrides

#### 3.1.1 Characterisation of tungsten oxynitride

Low temperature N<sub>2</sub> adsorption and desorption isotherms for the non-passivated tungsten oxynitride samples (Figure 1a) present a hysteresis and correspond to type IV. BET surface areas of 54, 42, 44 and 48 m<sup>2</sup> g<sup>-1</sup> were measured for samples W0, W5, W21 and W48, respectively. Interestingly, after an initial drop of the surface area, no further decrease is observed upon the progressive ageing of the samples, contrary to the previous reports.<sup>37-39</sup> In the present case, the maximum of the pore size distribution of the as-synthesised compound is centred around 5 nm (Figure 1b). After the exposure to air for 5 days, the maximum around 5 nm disappears, giving rise to two maxima centred around 3 and 7 nm, respectively. Upon ageing, the proportion of mesopores with 3 nm diameter increases, while pores with 7 nm diameter progressively disappear. Low temperature N<sub>2</sub> adsorption results could therefore indicate that exposure of the samples to the ambient air leads to a progressive decrease of the diameters of mesopores.

Table 3. Binding energies ( $E_b$ /eV) of W 4f peaks for samples W0-W48.

Sample	$W^{6+}$		$W^{5+}$	
	W 4f <sub>5/2</sub>	W 4f <sub>7/2</sub>	W 4f <sub>5/2</sub>	W 4f <sub>7/2</sub>
W0	37.8	35.6	34.5	32.5
W5	37.9	35.7	34.5	32.5
W21	38.0	35.8	34.5	32.5
W48	37.9	35.7	34.3	32.4

Table 4.  $W^{6+}/W^{5+}$  ratios calculated from the areas of the W 4f<sub>7/2</sub> peaks for samples W0-W48 (Figure 2).

Sample	$W^{6+}/W^{5+}$
W0	0.47
W5	0.75
W21	0.80
W48	0.70

The surface composition of the tungsten oxynitride samples are determined from their W 4f photoemission spectra, shown in Figure 2. Acceptable fits to the experimental data were obtained

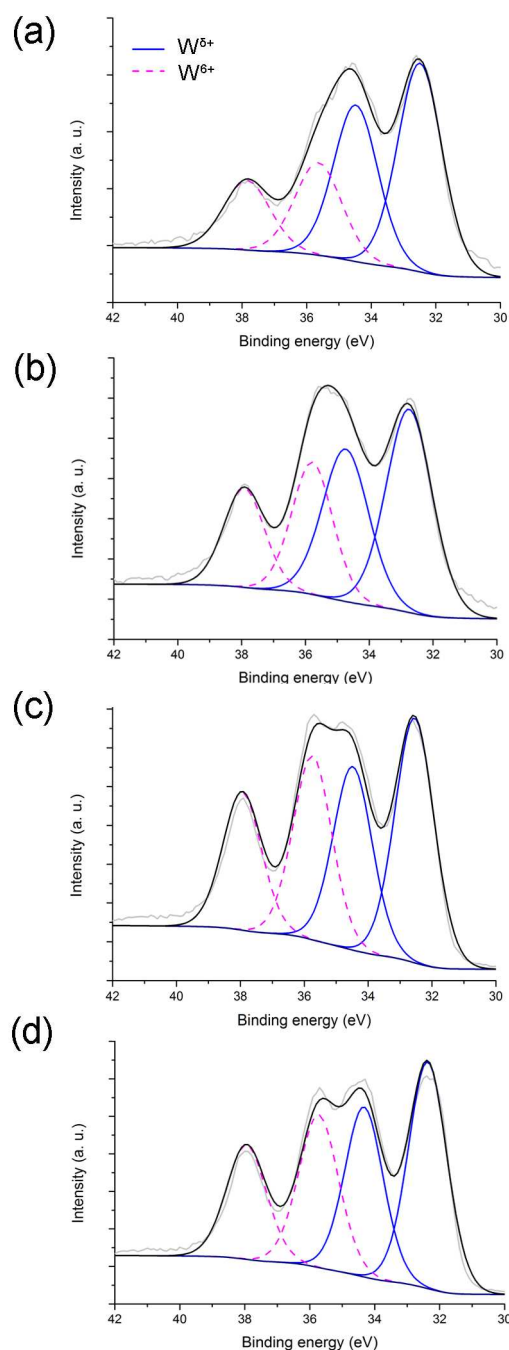


Figure 2. XPS spectra and W4f deconvolution peaks for W0 (a), W5 (b), W21 (c) and W48 (d) samples.

using two doublets, each with a separation of about 2 eV between the 4f<sub>7/2</sub> and 4f<sub>5/2</sub> component peaks (Table 3). The principal (4f<sub>7/2</sub>) peak of the doublet at higher binding energy is centred at approximately 35.7 eV for each sample, which is close to the range of values reported for WO<sub>3</sub>.<sup>37,42</sup> Consequently, this component is labelled W<sup>6+</sup>, and is evidence for the presence of tungsten trioxide. The 4f<sub>7/2</sub> peak of the doublet at lower binding energy is centred at approximately 32.5 eV, from which it is concluded that a second tungsten phase is also present on the sample surfaces: one with W in a

lower oxidation state. The identity of this phase is uncertain, as the measured binding energies fall between those reported for the

locations of predominant oxidation. Conflicting trends in the variations of the O/N ratio were observed in a number of attempted line scans. Comparing the results with the previously

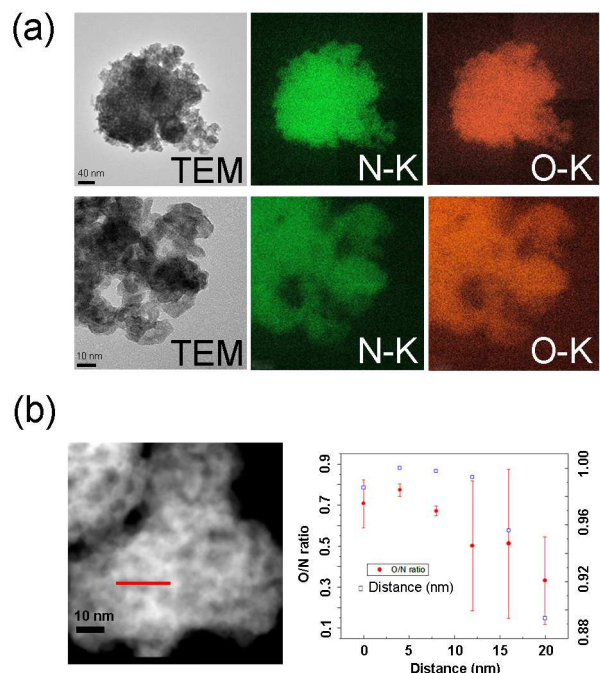


Figure 3. Bright-field TEM and the corresponding EFTEM maps of O and N elements (a) as well as a high-angle annular dark-field STEM image and the corresponding distribution of the O/N ratio (calculated from the electron energy loss data) along a line scan (in red) (b) for tungsten oxynitride sample exposed to air for 48 days.

mixed nitride,  $W_2N + WN$  (32.0 eV)<sup>37</sup>, and  $WO_2$  (33.0 eV),<sup>42</sup> and so the component is labelled  $W^{\delta+}$ , where  $\delta < 6$  (Figure 2). When comparing the  $W^{6+}/W^{\delta+}$  ratio for the fresh and aged samples (Table 4), it could be noted that upon exposure to air, the concentration of  $WO_3$  species on the surface increases. Interestingly, after an initial change of the  $W^{6+}/W^{\delta+}$  ratio from 0.47 to 0.75, no further significant increase of the ratio is observed. This result could indicate that tungsten oxynitride forms an oxide layer on the surface shortly after the exposure to the ambient air.

In order to investigate the oxidation of the surface of tungsten oxynitride samples in more detail, advanced TEM characterisation of the aged sample (W48) was attempted. Bright-field TEM (Figure 3a) as well as high-angle scanning transmission electron microscopy (STEM) images (Figure 3b) demonstrate that the material maintains the porous morphology after 48 days of exposure to the ambient air. EFTEM maps of oxygen and nitrogen (Figure 3a) indicate that these elements are distributed throughout the samples and therefore confirm that the synthesised material is the oxynitride, similar to the previously reported data for the fresh tungsten oxynitride.<sup>13</sup> Upon the analysis of the variations of the O/N ratio throughout the sample in the STEM mode (line scans), it could be observed that the distribution of O and N elements is not homogenous (Figure 3b). It is, however, not possible to determine the

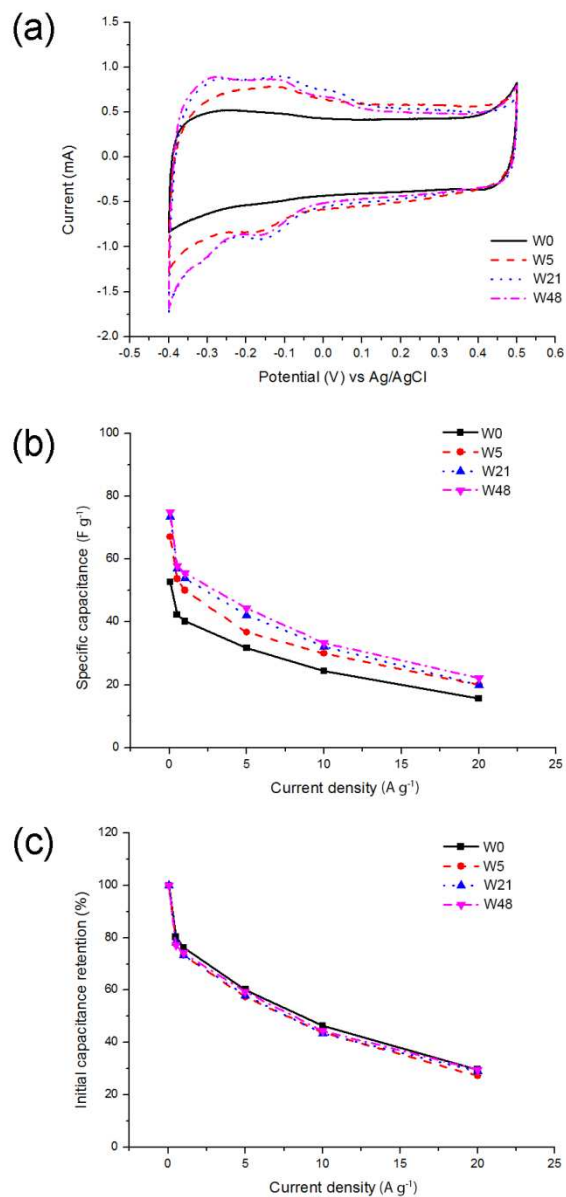


Figure 4. Influence of the ageing on the electrochemical performance of tungsten oxynitrides. Cyclic voltammetry measurements (a), rate capabilities (b) and rate capabilities normalised to the initial capacitance (c) for the fresh and aged tungsten oxynitrides.

reported TEM images of the as-synthesised tungsten oxynitride,<sup>13</sup> any obvious difference between the fresh and aged samples is difficult to argue. We have therefore concluded that the scale of changes upon ageing occurs within a fine range of about 1 nm and could not be monitored reliably with the TEM equipment available to us.

### 3.1.2 Electrochemical properties of tungsten oxynitride

Cyclic voltammetry (CV) curves of tungsten oxynitride samples in 1M H<sub>2</sub>SO<sub>4</sub> electrolyte (Figure 4a) show a nearly ideal rectangular CV curve for the as-synthesised sample (W0), with the operating potential window of 0.9 V, between -0.4 and 0.5 V vs Ag/AgCl. Upon exposure to ambient air, reversible

The shape of the galvanostatic charge and discharge curves (Figure 5a) is close to triangular for all samples, with an increased IR drop measured at a higher current load (Figure 5b). It could, however, be observed that the ageing of tungsten oxynitride leads to a decrease of the Coulombic efficiency, which could be seen from the distortion of the shape of CV curves of the aged samples as well (Figure 4a). In fact, the

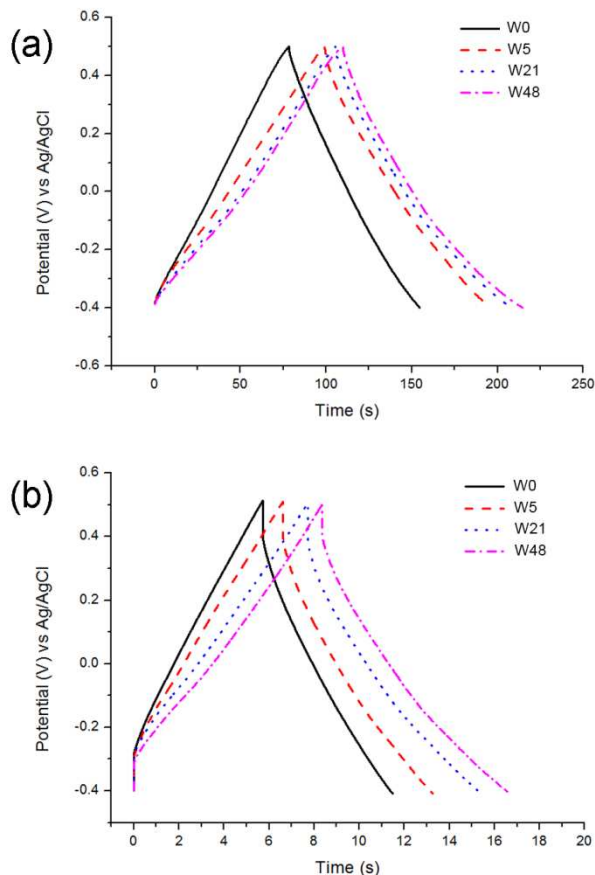


Figure 5. Galvanostatic charge and discharge curves of tungsten oxynitride samples at the current load of 0.5 A g<sup>-1</sup> (a) and 5 A g<sup>-1</sup> (b).

redox peaks could be observed in cyclic voltammograms around -0.1 V for samples W5-W48, resembling the peaks observed for the amorphous, mesoporous tungsten oxide.<sup>43</sup> This result is consistent with XPS measurements indicating the increase of WO<sub>3</sub> concentration on the surface of tungsten oxynitride. It could also be noted that the specific capacitance, measured by galvanostatic charge and discharge tests, increases from 57 F g<sup>-1</sup> (106 μF cm<sup>-2</sup>) for the fresh sample (W0) to 75 F g<sup>-1</sup> (156 μF cm<sup>-2</sup>) for the sample exposed to air for 48 days (W48). Interestingly, this increase of the capacitance is not accompanied by the fade of the rate capability (Figure 4b), indicating that the intrinsic conductivity is not affected by the ageing of the samples. In fact, for the fresh sample (W0), 29.6 % of the initial capacitance is retained upon increasing the current load from 0.05 to 20 A g<sup>-1</sup> (400-fold). The exact same value is calculated for the sample exposed to air for 48 days (W48) (Figure 4c).

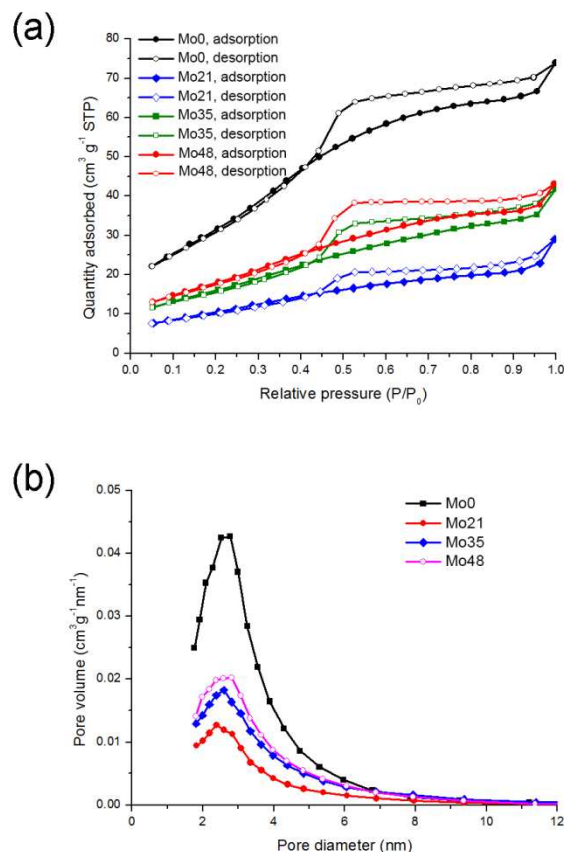


Figure 6. Nitrogen adsorption and desorption isotherms (a) and pore size distributions (b) for molybdenum oxynitride samples.

Coulombic efficiency calculated from the galvanostatic charge and discharge curves at the current load of 0.05 A g<sup>-1</sup> decreases from 94% for W0 to only 77% for W48. The changes in the shapes of the electrochemical curves and the decreased Coulombic efficiency may be related to water splitting and hydrogen evolution developing close to -0.4 V vs. Ag/AgCl. Overall, it can be concluded that the progressive change of the oxide layer composition over time leads to an increase in the specific capacitance, while the rate capability, which is defined by the conductivity of the sample, remains the same as the bulk of the sample is not affected by the exposure to air. The ageing, however, degrades the Coulombic efficiency, indicating a presence of irreversible processes.

### 3.1.3 Characterisation of molybdenum oxynitride

N<sub>2</sub> adsorption isotherms for molybdenum oxynitride samples possess a hysteresis (Figure 6a) and correspond to type IV, typical for mesoporous materials. Surface areas of 123, 39, 60 and 67 m<sup>2</sup> g<sup>-1</sup> are measured for samples Mo0, Mo21, Mo35 and Mo48, respectively. Interestingly, after the initial drop from 123 to 39 m<sup>2</sup> g<sup>-1</sup>, an increase of the surface area is observed upon progressive ageing. The maximum of the pore size distribution is centred around 3 nm (Figure 6b). However, as opposed to tungsten oxynitride, no apparent shift of the

Figure 7. XPS spectra and Mo 3d deconvolution peaks for Mo0 (a), Mo21 (b), Mo35 (c) and Mo48 (d) samples.

Table 5. Binding energies ( $E_b$ /eV) of Mo 3d peaks for samples Mo0-Mo48.

Sample	Mo <sup>6+</sup>		Mo <sup>5+</sup>	
	Mo 3d <sub>3/2</sub>	Mo 3d <sub>5/2</sub>	Mo 3d <sub>3/2</sub>	Mo 3d <sub>5/2</sub>
Mo0	235.5	232.4	231.8	228.7
Mo21	235.7	232.6	231.8	228.7
Mo35	235.8	232.7	231.8	228.7
Mo48	235.8	232.7	231.8	228.7

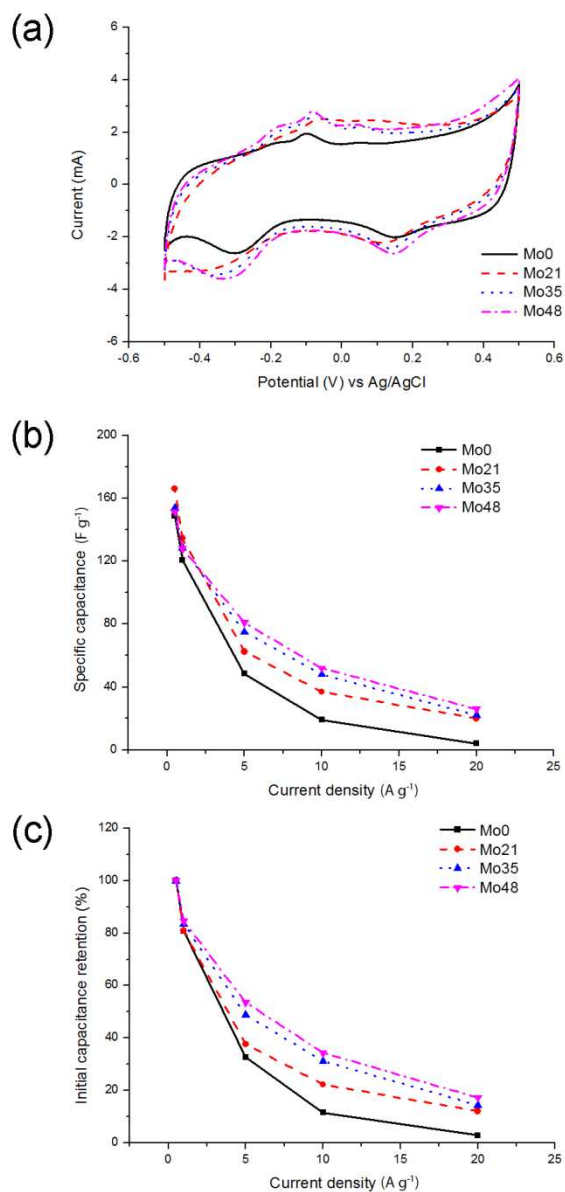
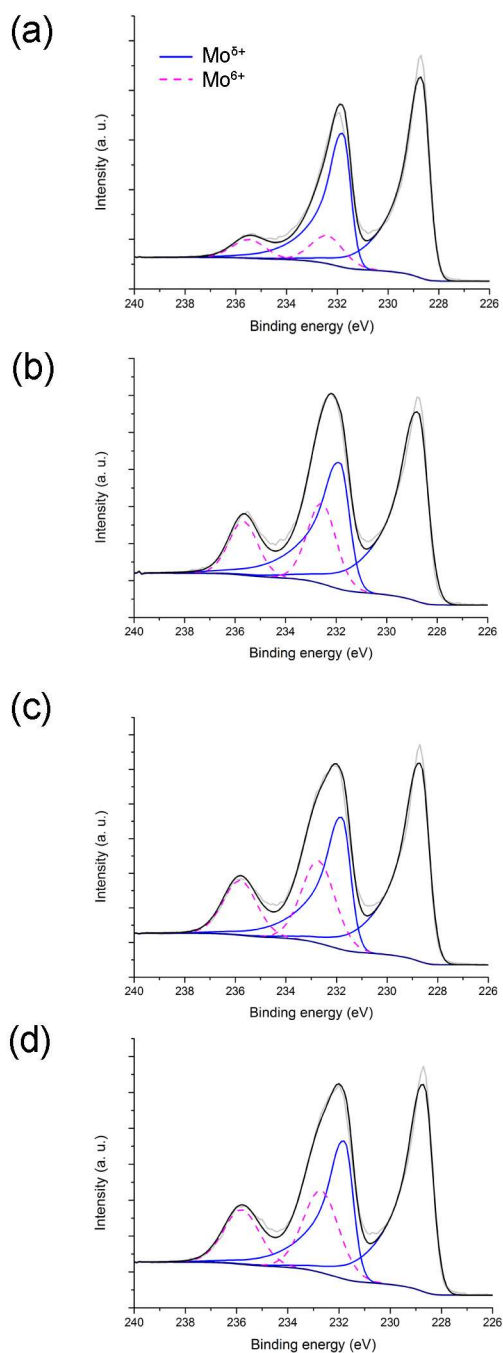


Figure 8. Influence of the ageing on the electrochemical performance of molybdenum oxynitrides. Cyclic voltammograms (a), rate capabilities (b) and rate capabilities normalised to the initial capacitance (c) for the fresh and aged molybdenum oxynitrides.



Table 6.  $\text{Mo}^{6+}/\text{Mo}^{\delta+}$  ratios calculated from the areas of the Mo  $3d_{5/2}$  peaks for samples Mo0-Mo48 (Figure 7).

Sample	$\text{Mo}^{6+}/\text{Mo}^{\delta+}$
Mo0	0.15
Mo21	0.33
Mo35	0.42
Mo48	0.42

maximum is observed for molybdenum oxynitride upon exposure of the sample to the ambient air.

Mo 3d spectra of the molybdenum oxynitrides are shown in Figure 7. These, like the W 4f spectra of the tungsten analogues, are fitted with two doublets, with that at higher binding energy having a  $3d_{5/2}$  peak centred between

component located at 228.7 eV for all four samples. In several earlier reports of XPS data acquired for Mo oxynitrides, this asymmetry has been modelled by fitting two peaks, separated by about 1 eV, to each component, and assigning these to additional Mo phases: one containing the  $\text{Mo}^{4+}$  ion, and another with Mo in a lower, but indeterminate, oxidation state, designated  $\text{Mo}^{\delta+}$ .<sup>47-49</sup> An alternative explanation is that the doublet is associated with a single Mo species, with an oxidation state lower than that of  $\text{Mo}^{\text{VI}}$ , and that the asymmetry is a consequence of multiplet splitting; that is, of the interaction of unpaired 4d electrons with the 3d hole. Such an explanation has been given for the asymmetry observed in the Mo 3d spectrum of  $\text{MoO}_2$ .<sup>44</sup> Which of these two possibilities properly describes the Mo oxynitrides in this study cannot be resolved from the XPS data alone, and so for the spectra in Figure 7, each component of the doublet at lower binding energy is fitted with a single asymmetric peak, labelled  $\text{Mo}^{\delta+}$ , representing the contribution from *at least* one Mo species with  $0 < \delta \leq 4$ . The  $\text{Mo}^{6+}/\text{Mo}^{\delta+}$  ratios (Table 6) increase for the samples exposed to air, indicating the progressive oxidation, from 0.15 for the sample Mo0 to 0.42 for the sample Mo35. There appears to be no change after 35 days.

### 3.1.4 Electrochemical properties of molybdenum oxynitride

Electrochemical characterisation of molybdenum oxynitride samples (Figure 8) shows the operating potentials between -0.5 to 0.5 V vs Ag/AgCl in 1M  $\text{H}_2\text{SO}_4$  electrolyte and multiple redox peaks present on the surface of the cyclic voltammetry curves (Figure 8a). The maximum specific capacitance of  $149 \text{ F g}^{-1}$  ( $121 \mu\text{F cm}^{-2}$ ) is measured for the fresh sample (Mo0) while for the sample exposed to air (Mo48), this value is  $152 \text{ F g}^{-1}$  ( $227 \mu\text{F cm}^{-2}$ ), indicating an increase of the specific capacitance per unit of electrode area. As opposed to tungsten oxynitride, the ageing has an effect on the rate capability (Figure 8 b, c). Upon increase of the current load from  $0.5$  to  $20 \text{ A g}^{-1}$ , the fresh sample shows a significant drop in the specific capacitance, with only 2.7 % of the initial capacitance remaining at  $20 \text{ A g}^{-1}$

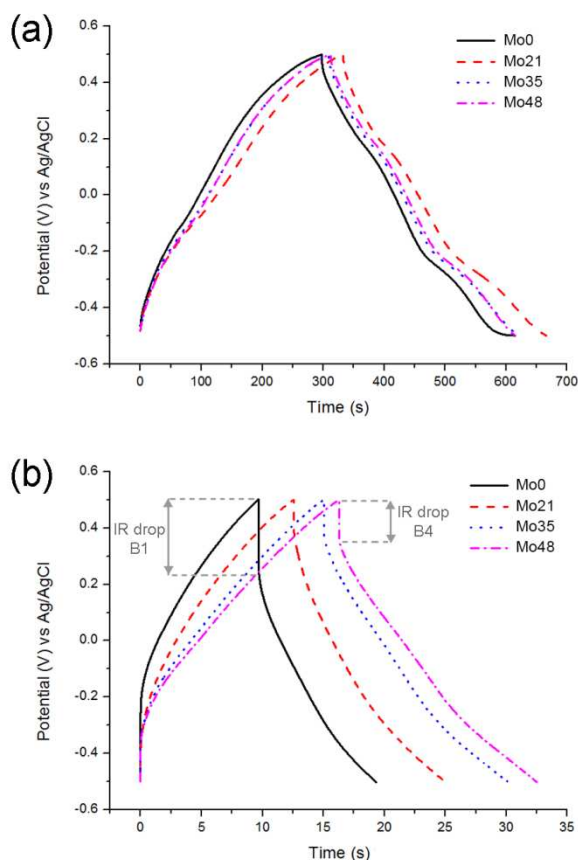


Figure 9. Glavanostatic charge and discharge curves of molybdenum oxynitride samples at the current load of  $0.5 \text{ A g}^{-1}$  (a) and  $5 \text{ A g}^{-1}$  (b). The difference in the IR drop between the fresh (Mo0) and aged (Mo48) samples is highlighted for the higher current load (b).

232.5 and 232.7 eV (Table 5). This is within the range of values reported for  $\text{MoO}_3$ ,<sup>44-47</sup> and so the component is assigned to the  $\text{Mo}^{6+}$  ion. The two peaks of the doublet at lower binding energy have a pronounced asymmetry, with the maximum of the  $3d_{5/2}$

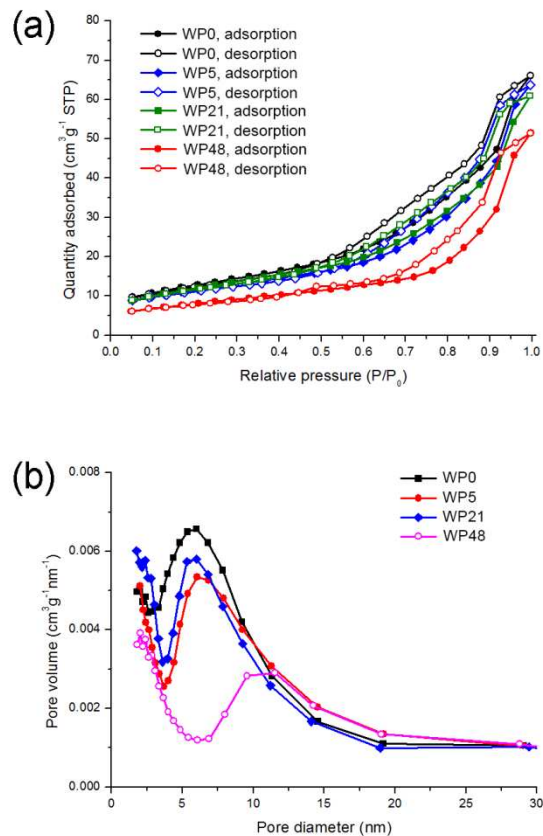


Figure 10. Low temperature adsorption isotherms (a) and pore size distributions (b) of the passivated tungsten oxynitride samples exposed to air for different periods.

(Figure 8c). After exposure to air for 48 days, the rate capability increases progressively and reaches 17.2 % of the initial capacitance retention for the sample (Mo48).

When comparing the shapes of galvanostatic charge and discharge curves of molybdenum oxynitride samples (Figure 9), no apparent difference is observed at the current load of  $0.5 \text{ A g}^{-1}$  (Figure 9a). At the higher current load, however, it can be noted that the IR drop for the aged sample (Mo48) decreases significantly when compared to the fresh sample (Mo0) (Figure 89). This could indicate faster kinetics of the electrochemical processes for the sample Mo48.

### 3.2 Effect of the passivation on the ageing: comparison of the passivated and non-passivated tungsten oxynitride samples

In order to study the effect of passivation on the ageing, passivated tungsten oxynitride samples exposed to ambient air for different periods (WP0-WP48) are characterised by low temperature nitrogen adsorption (Figure 10) and XPS measurements (Figure 11). The as-synthesised, passivated tungsten oxynitride sample (WP0) presents a type IV low temperature  $\text{N}_2$  adsorption isotherm (Figure 10a). The maximum of the pore size distribution is, however, shifted towards higher values and is centred around 7 nm (Figure 10b).

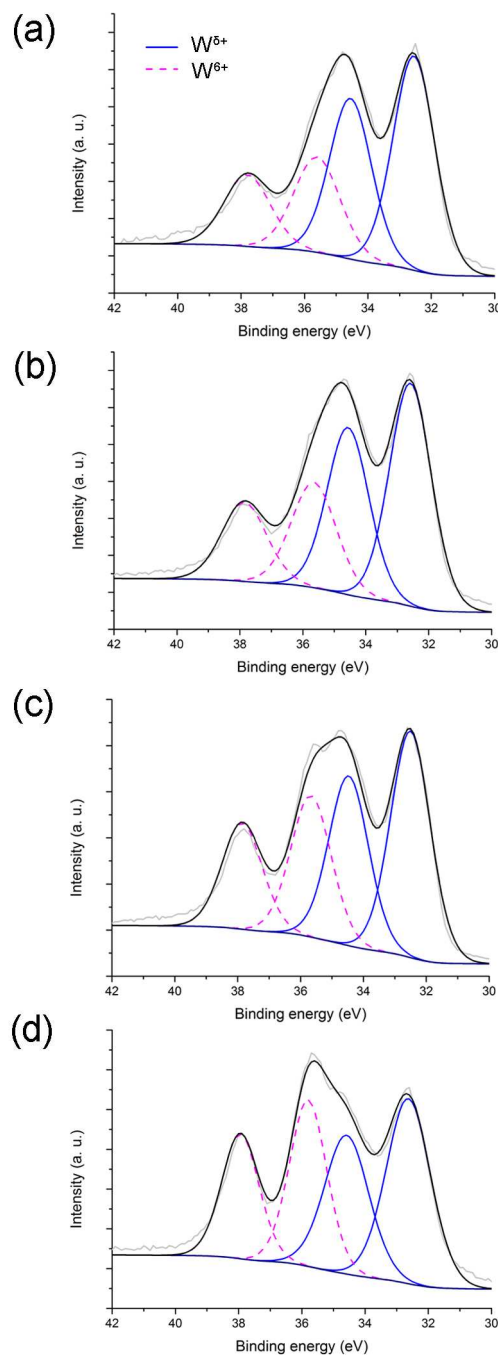


Figure 11. XPS spectra and W4f deconvolution peaks for WP0 (a), WP5 (b), WP21 (c) and WP48 (d) samples.

Furthermore, the shape of the isotherm is different from the one reported for samples W0-W48 (Figure 1). Upon ageing, the maximum of the pore size distribution shifts towards higher values, and reaches approximately 12 nm (Figure 10b), possibly indicating the blockage of the smaller pores upon the room temperature oxidation. The specific surface areas for the samples WP0, WP5, WP21 and WP48, calculated with BET method, are  $44.6$ ,  $40.1$ ,  $42.3$  and  $28.5 \text{ m}^2 \text{ g}^{-1}$ , respectively. This decrease in the surface areas, different from the non-passivated samples (Figure 1), is similar to the previously reported data,

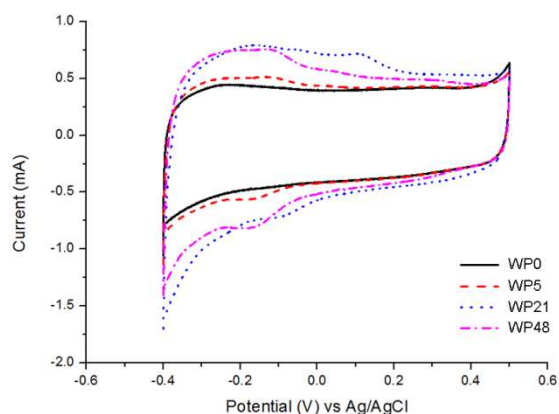


Figure 12. Cyclic voltammograms of the passivated tungsten oxynitride samples measured with the scan rate of  $5 \text{ mV s}^{-1}$ .

where the surface area of the passivated tungsten oxynitride decreased to  $30 \text{ m}^2 \text{ g}^{-1}$  after the exposure to air for 40 days.<sup>37</sup> These differences between the passivated and non-passivated tungsten oxynitrides indicate that passivation could have an influence on the structure of the pores.

Table 7. Binding energies ( $E_b/\text{eV}$ ) of W 4f peaks for samples WP0-WP48.

Sample	$\text{W}^{6+}$		$\text{W}^{\delta+}$	
	W 4f <sub>5/2</sub>	W 4f <sub>7/2</sub>	W 4f <sub>5/2</sub>	W 4f <sub>7/2</sub>
WP0	37.8	35.6	34.5	32.5
WP5	37.9	35.6	34.6	32.6
WP21	37.9	35.7	34.5	32.5
WP48	37.9	35.8	34.6	32.6

Table 8.  $\text{W}^{6+}/\text{W}^{\delta+}$  ratios calculated from the areas of the W 4f<sub>7/2</sub> peaks for samples WP0-WP48 (Figure 11).

Sample	$\text{W}^{6+}/\text{W}^{\delta+}$
WP0	0.49
WP5	0.51
WP21	0.64
WP48	0.76

W 4f spectra of the passivated tungsten oxynitride samples (Figure 11), like those of the non-passivated samples (Figure 2), are each composed of two doublets, attributed to  $\text{W}^{6+}$  and  $\text{W}^{\delta+}$  (Table 7). The relative ratios of these are listed in Table 8, from which it is evident that this ratio increases steadily with ageing. When comparing the ratios of  $\text{W}^{6+}$  and  $\text{W}^{\delta+}$  species for the non-passivated (W0-W48) and passivated (WP0-WP48) samples, it could be observed that for the as-synthesised tungsten oxynitrides, this ratio is slightly lower for W0 (0.47) when compared to WP0 (0.49) (refer to Table 4 and Table 8). Upon ageing, the  $\text{W}^{6+}/\text{W}^{\delta+}$  ratio for samples W5-W48 increases sharply after the exposure to air for only five days and

reaches a saturation (Table 4), while for the passivated samples, a progressive increase is observed (Table 8). For samples W48

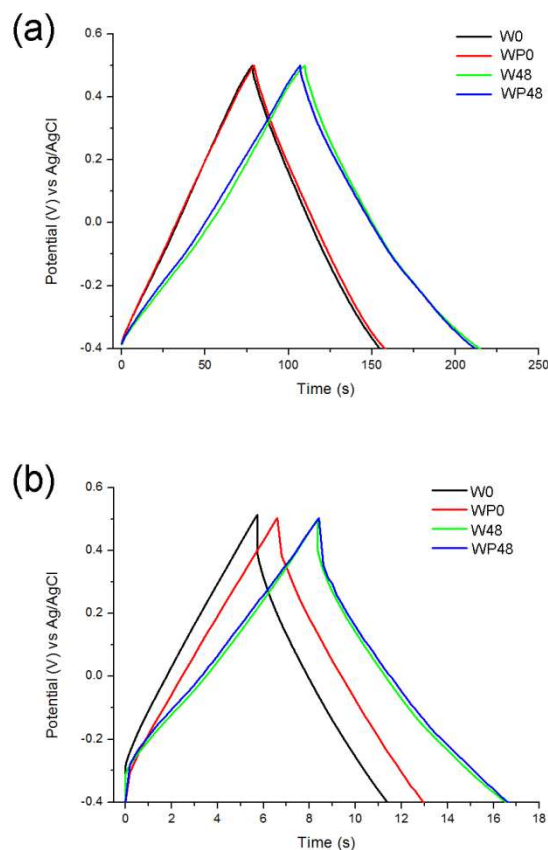


Figure 13. Comparison of the galvanostatic charge and discharge curves of the non-passivated and passivated tungsten oxynitride samples at the current load of  $0.5 \text{ A g}^{-1}$  (a) and  $5 \text{ A g}^{-1}$  (b).

and WP48 the  $\text{W}^{6+}/\text{W}^{\delta+}$  ratios are 0.70 and 0.76, respectively. These results could indicate that although the passivation of the synthesised tungsten oxynitride slows down the oxidation in the ambient air, it does not prevent it.

Cyclic voltammetry measurements of the passivated tungsten oxynitride samples exposed to air for different periods (Figure 12) indicate a nearly ideal rectangular shape of the CV curves for the freshly synthesised samples. Upon ageing, reversible redox peaks start to appear around  $-0.1 \text{ V}$ , similar to the results observed for the non-passivated samples (Figure 4a). This distortion of the CV shapes for both passivated and non-passivated materials upon exposure to air correlates with XPS results, and indicates that the passivation does not prevent the increase of the amount of tungsten oxide on the surface of the materials, which leads to changes in their electrochemical properties.

When comparing the galvanostatic charge and discharge behaviour of the fresh and aged samples at different current loads (Figure 13), the curves of the passivated and non-passivated samples nearly superpose at the current load of  $0.5 \text{ A g}^{-1}$  (Figure 13 a). The specific capacitance values of the as-

synthesised samples (W0 and WP0) are 42.3 and 43.6 F g<sup>-1</sup>, respectively. Upon ageing, the specific capacitance values

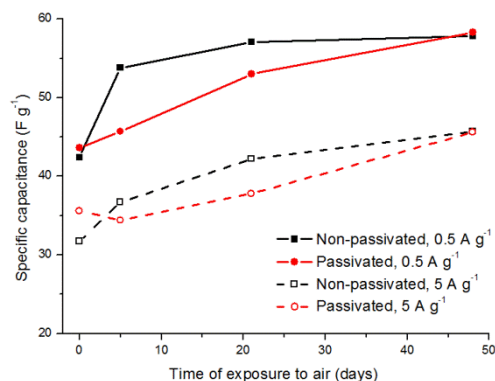


Figure 14. Comparison of the specific capacitance values for the passivated and non-passivated tungsten oxynitride samples exposed to air for different periods at the current loads of 0.5 and 5 A g<sup>-1</sup>.

increase to 57.8 and 58.3 F g<sup>-1</sup> for samples W48 and WP48, respectively. At a higher current load of 5 A g<sup>-1</sup> (Figure 13 b), although the as-synthesised, passivated sample (WP0) demonstrates a slightly higher specific capacitance value of 35.6 F g<sup>-1</sup> when compared to the non-passivated sample (31.7 F g<sup>-1</sup>), both of the aged samples show similar capacitance values of 44.4 F g<sup>-1</sup> and 44.2 F g<sup>-1</sup> for W48 and WP48, respectively.

The progressive changes of the specific capacitance values for the passivated and non-passivated tungsten oxynitride samples with time are depicted on figure 14. For the non-passivated samples, a sharp increase of the specific capacitance is observed after five days of exposure to air at the current loads of 0.5 and 5 A g<sup>-1</sup>, followed by a plateau. For the passivated samples, a different behaviour is observed, with the specific capacitance values increasing progressively with time. After 48 days of exposure, however, both non-passivated and passivated samples reach similar specific capacitance values. These results indicate that the change in the electrochemical properties of the non-passivated samples happens soon after exposure to air, followed by the saturation, while for the passivated samples, these changes occur progressively, thus correlating with XPS measurements.

#### 4. Discussion

Results presented in this work demonstrate that properties of molybdenum and tungsten oxynitrides are changing with time upon exposure to the ambient air. More specifically, an increase of the amount of the oxide species on their surface is observed from the XPS measurements, while changes in the surface areas and pore size distributions are measured with the low temperature N<sub>2</sub> adsorption. The progressive oxidation of the surface leads to significant variations of the electrochemical properties when transition metal oxynitrides are used as active electrode materials for supercapacitors. For instance, for

tungsten oxynitrides, although an increase of the specific capacitance is observed upon exposure to air, ageing leads to the distortion of the cyclic voltammetry curves, and decreases the Coulombic efficiencies. For molybdenum oxynitrides, however, an increase of the rate capability is observed. These results indicate that ageing is material-specific and could lead to different consequences: the presence of irreversible electrochemical processes, as it is the case with tungsten oxynitride, or an improvement of the rate capability, as it is the case with molybdenum oxynitride. It could therefore be recommended, in view of applications of transition metal nitrides and oxynitrides in the energy conversion and storage devices, to evaluate the influence of the ageing on the properties of a specific compound in order to select the optimal storage conditions (controlled ageing or storage in an inert gas atmosphere).

Passivation of transition metal oxynitrides prior the exposure to air after the temperature-programmed reduction is a common practice, and it is performed in order to avoid the oxidation of the samples. Results presented in this article demonstrate that although the passivation has an effect on the properties of the as-synthesised samples and slows down the oxidation in the ambient air, it does not prevent the ageing. In fact, after long storage periods, both passivated and non-passivated tungsten oxynitride samples show similar changes in the properties and electrochemical behaviour. It could therefore be suggested to perform the passivation when ageing leads to degradation of the electrochemical performance in order to slow down this process.

In summary, results presented in this work demonstrate that passivation prior exposure to air as well as storage conditions of transition metal oxynitrides have a significant influence on their electrochemical properties. It is therefore recommended to evaluate and carefully control these parameters when using transition metal oxynitrides in the energy conversion and storage devices. Otherwise, ageing could affect the electrochemical performance, the reproducibility of the measurements, or the comparison of the results to data reported in the literature.

#### Conclusions

In this article, ageing of molybdenum and tungsten oxynitrides is explored, and its influence on their electrochemical properties in supercapacitors is investigated. Results indicate that upon ageing, the progressive oxidation of the samples leads to material-specific changes of the electrochemical properties. For tungsten oxynitride, for instance, ageing leads to an increase of the specific capacitance but decreases the Coulombic efficiency, while for molybdenum oxynitride, an improvement of the rate capability is observed. Furthermore, it is demonstrated that although the passivation of the samples prior the exposure to air slows down the ageing, it does not prevent it. Recommendations are therefore made regarding the preparation and storage conditions of transition metal oxynitrides.

## Acknowledgements

This research project is supported by the ARC Centre of Excellence for Functional Nanomaterials, an ARC Discovery grant and a grant from Deakin University (Central Research Grant Scheme). The authors thank Prof Yuri Gogotsi (Drexel University) for helpful discussions, Mr Robert Lovett for his help with technical matters and Mr Mengqi Zhou with his help with some Figures. The authors acknowledge the use of the XPS facilities in the Victorian Node of the Australian National Fabrication Facility (ANFF).

## Notes and references

<sup>a</sup> Institute for Frontier Materials (IFM), Deakin University, Waurn Ponds VIC 3216, Australia. Fax: +61 3 5227 1103; Tel: +61 3 5227 2931; E-mail: alexey.glushenkov@deakin.edu.au

<sup>b</sup> Centre for Materials and Surface Science, Department of Physics, La Trobe University, VIC 308, Australia. Fax: +6139479 1552; Tel: +613 9479 2646; E-mail: R.Jones@latrobe.edu.au

<sup>c</sup> School of Physics and Centre for Research on Adaptive Nanostructures and Nanodevices (CRANN), Trinity College Dublin, Dublin 2, Ireland. Fax: +353 1 896 3033; Tel: +353 1 896 4655; E-mail: hozhang@tcd.ie

<sup>d</sup> Melbourne Centre for Nanofabrication, 151 Wellington Rd, Clayton, VIC 3168, Australia

- S. Dong, X. Chen, X. Zhang and G. Cui, *Coord. Chem. Rev.*, 2013, **257**, 1946;
- B. Das, M. V. Reddy, G. V. Subba Rao and B. V. R. Chowdari, *RSC Adv.*, 2012, **2**, 9022;
- B. Das, M. V. Reddy, G. V. Subba Rao and B. V. R. Chowdari, *J. Mater. Chem.*, 2012, **22**, 17505;
- B. Das, M. V. Reddy, P. Malar, T. Osipowicz, G. V. Subba Rao and B. V. R. Chowdari, *Solid State Ionics*, 2009, **180**, 1061;
- B. Das, M. V. Reddy and B. V. R. Chowdari, *Nanoscale*, 2013, **5**, 1961;
- Q. Sun and Z.-W. Fu, *Electrochim. Acta*, 2008, **54**, 403;
- Q. Sun and Z.-W. Fu, *Electrochim. Solid-State Lett.*, 2007, **10**, A189;
- Z.-W. Fu, Y. Wang, X.-L. Yue, S.-L. Zhao and Q.-Z. Qin, *J. Phys. Chem. B*, 2004, **108**, 2236;
- S. Bouhtiyaa, R. Lucio Porto, B. Laïk, P. Boulet, F. Capon, J. P. Pereira-Ramos, T. Brousse and J. F. Pierson, *Scripta Mater.*, 2013, **68**, 659;
- Q. Sun and Z.-W. Fu, *Appl. Surf. Sci.*, 2012, **258**, 3197;
- Y.-N. Zhou, C. Liu, H.-J. Chen, L. Zhang, W.-J. Li and Z.-W. Fu, *Electrochim. Acta*, 2011, **56**, 5532;
- A. M. Glushenkov, D. Hulicova-Jurcakova, D. Llewellyn, G. Q. Lu and Y. Chen, *Chem. Mater.*, 2010, **22**, 914;
- O. Kartachova, A. M. Glushenkov, Y. Chen, H. Zhang, X. J. Dai and Y. Chen, *J. Power Sources*, 2012, **220**, 298;
- O. Kartachova, A. M. Glushenkov, Y. Chen, H. Zhang and Y. Chen, *J. Mater. Chem. A*, 2013, **1**, 7889;
- X. Zhou, C. Shang, L. Gu, S. Dong, X. Chen, P. Han, L. Li, J. Yao, Z. Liu, H. Xu, Y. Zhu and G. Cui, *ACS Appl. Mater. Interfaces*, 2011, **3**, 3058;
- M. Wixom, L. Owens, J. Parker, J. Lee, I. Song and L. Thompson, in *Proceedings of the Symposium on Electrochemical Capacitors II*, 1997, **96**, 63;
- S. Dong, X. Chen, L. Gu, X. Zhou, H. Xu, H. Wang, Z. Liu, P. Han, J. Yao, L. Wang, G. Cui and L. Chen, *ACS Appl. Mater. Interfaces*, 2011, **3**, 93;
- D. Choi and P. N. Kumta, *J. Electrochem. Soc.*, 2006, **153**, A2298;
- C. Z. Deng and K. C. Tsai, in *Proceedings of the Symposium on Electrochemical Capacitors II*, ed. M. F. Delnick, Electrochemical Society, Pennington, 1997, vol. 96-25, pp. 75-84;
- X.-L. Li, Y. Xing, H. Wang, H.-L. Wang, W.-D. Wang and X.-Y. Chen, *Trans. Nonferrous Met. Soc. China*, 2009, **19**, 620;
- A.-R. Ko, S.-B. Han, Y.-W. Lee and K.-W. Park, *Phys. Chem. Chem. Phys.*, 2011, **13**, 12705;
- P. Pande, P. G. Rasmussen and L. T. Thompson, *J. Power Sources*, 2012, **207**, 212;
- X. Zhou, H. Chen, D. Shu, C. He and J. Nan, *J. Phys. Chem. Solids*, 2009, **70**, 495;
- F. Cheng, C. He, D. Shu, H. Chen, J. Zhang, S. Tand and D. E. Finlow, *Mater. Chem. Phys.*, 2011, **131**, 268;
- D. Choi and P. N. Kumta, *J. Am. Ceram. Soc.*, 2007, **90**, 3113;
- D. Choi, G. E. Blomgren and P. N. Kumta, *Adv. Mater.*, 2006, **18**, 1178;
- M. Wu, Q. Zhang, J. Xiao, C. Ma, X. Lin, C. Miao, Y. He, Y. Gao, A. Hagfeldt and T. Ma, *J. Mater. Chem.*, 2011, **21**, 10761;
- Y. Wang, M. Wu, X. Lin, Z. Shi, A. Hagfeldt and T. Ma, *J. Mater. Chem.*, 2012, **22**, 4009;
- G. R. Li, J. Song, G. L. Pan and X. P. Gao, *Energy Environ. Sci.*, 2011, **4**, 1680;
- Y. Wang, R. Ohnishi, E. Yoo, P. He, J. Kubota, K. Domen and H. Zhou, *J. Mater. Chem.*, 2012, **22**, 15549;
- P. He, Y. Wang and H. Zhou, *Chem. Commun.*, 2011, **47**, 10701;
- R. Ohnishi, K. Takanabe, M. Katayama, J. Kubota and K. Domen, *J. Phys. Chem. C*, 2013, **117**, 496;
- A. Ishihara, S. Doi, S. Mitsushima and K.-I. Ota, *Electrochim. Acta*, 2008, **53**, 5442;
- H. Tominaga and M. Nagai, *Electrochim. Acta*, 2009, **54**, 6732;
- C. Pozo-Gonzalo, O. Kartachova, A. A. J. Torriero, P. C. Howlett, A. M. Glushenkov, D. M. Fabijanic, Y. Chen, S. Poissonnet and M. Forsyth, *Electrochim. Acta*, 2013, **103**, 151;
- K. Zhang, L. Zhang, X. Chen, X. He, X. Wang, S. Dong, P. Han, C. Zhang, S. Wang, L. Gu and G. Cui, *J. Phys. Chem. C*, 2013, **117**, 858;
- D.-H. Cho, T.-S. Chang and C.-H. Shin, *Catal. Lett.*, 2000, **67**, 163;
- X. Goin, R. Marchand, P. L'Haridon and Y. Laurent, *J. Solid State Chem.*, 1994, **109**, 175;
- C. Sayag, G. Bugli, P. havil and G. Djéga-Mariadassou, *J. Catal.*, 1997, **167**, 372;
- M. R. Lukatskaya, O. Mashtalir, C. E. Ren, Y. Dall'Agnese, P. Rozier, P. L. Taberna, M. Naguib, P. Simon, M. W. Barsoum and Y. Gogotsi, *Science*, 2013, **341**, 1502;
- J. Chastain (ed.), *Handbook of X-ray Photoelectron Spectroscopy*, Perkin-Elmer Corp., Minnesota, USA, 1992;
- J. F. Morar, F. J. Himpsel, G. Hughes, J. L. Jordan, and F. R. McFeely, *J. Vac. Sci. Technol. A*, 1985, **3**, 1477.

## Journal Name

- 43 C. Jo, I. Hwang, J. Lee, C. W. Lee and S. Yoon, *J. Phys. Chem. C*, 2011, **115**, 11880;
- 44 F. Werfel, E. Minni, *J. Phys. C: Solid State Phys.*, 1983, **16**, 6091–6100.
- 45 L. D. Lopez-Carreno, G. Benitez, L. Viscido, J. M. Heras, J. M. Yubero, J. P. Espinos, A. R. Gonzalez-Eliphe, *Surf. Interface Anal.*, 1998, **26**, 235.
- 46 C.-O. A. Olsson, H.-J. Mathieu, D. Landolt, *Surf. Interface Anal.*, 2002, **34**, 130.
- 47 Z. B. Wei, P. Grange and B. Delmon, *Appl. Surf. Sci.*, 1998, **135**, 107;
- 48 Y. Zhang, Q. Xin, I. Rodriguez-Ramos and A. Guerrero-Ruiz, *Mater. Res. Bull.*, 1999, **34**, 145;
- 49 J.-G. Choi, J. R. Brenner, C. W. Colling, B. G. Demczyk, J. L. Dunning and L. T. Thompson, *Catal. Today*, 1992, **15**, 201.